Gemini-Enabled Sub-Hertz Elastic FWI for Robust Subsalt Velocity Model Building

Hao Xing, Richard Huang, Zhuoquan Yuan, Khaled Abdelaziz, Carsten Udengaard, Aurora R. Castelan, Mohammed Hegazy (TGS)*

Summary

In this study, we demonstrate how the convergence of advanced acquisition (sub-Hertz Gemini source) and robust inversion (Elastic Dynamic Matching FWI, E-DMFWI) significantly expands initial model tolerance, enables salt reconstruction directly from sediment-flood models, and stabilizes subsalt velocity updates. Field examples from multiple Amendment surveys illustrate that starting FWI at 0.6 Hz improves background velocity recovery, intra-salt resolution, and subsalt imaging coherence compared with conventional 1.6 Hz workflows. The results highlight that acquisition–imaging integration is essential for next-generation subsalt exploration.

Introduction

Full-waveform inversion (FWI) iteratively updates subsurface velocity models by minimizing the misfit between synthetic and observed seismic data. Despite its theoretical completeness, FWI is highly sensitive to cycle skipping, which occurs when phase differences exceed half a wavelength. Successful inversion is governed by four factors: wavelet fidelity, initial velocity model accuracy, low-frequency content of the data, and robustness of the objective function. In the Gulf of America, legacy velocity workflows relied on streamer-based top-down tomography with sediment flood and salt flood migration. This approach often produces errors in salt geometry and subsalt velocities due to limited illumination and restricted angles.

Recent acquisition advances have changed this paradigm. Sparse-node OBN geometries provide ultra-long offsets, while the Gemini single-chamber source delivers usable energy below 1 Hz. Compared to conventional air-gun arrays, the Gemini source provides ~15 dB improvement at 1 Hz and coherent phase energy down to 0.6 Hz (Figure 1) (Cvetkovic, et. al., 2025). Simplified point-source behavior further improves numerical simulation fidelity in FWI. Concurrently, Dynamic Matching FWI (DMFWI) replaces global L2 minimization with localized time–space dynamic matching operators, improving robustness in high-gradient media such as salt boundaries (Mao, et. al., 2020, Xing, et. al., 2025). Elastic DMFWI (E-DMFWI) extends this framework to multi-component elastic wavefields, preserving waveform coherency across P, S, multiples, and mode conversions (Macesanu, et. al., 2024, Liu, et. al., 2025).

This paper evaluates how ultra-low frequency acquisition combined with elastic dynamic matching inversion improves subsalt imaging.

Case Studies

Ultra-Low Frequency and Initial Model Tolerance

One of the fundamental limitations of FWI in complex salt provinces is its sensitivity to inaccuracies in the initial velocity model. In high-contrast environments such as the Gulf of America, even modest background velocity bias can rapidly lead to cycle skipping, particularly when inversion is initiated at frequencies above 1 Hz. The convergence basin of conventional least-squares FWI narrows dramatically as frequency increases, making the inversion highly dependent on the kinematic fidelity of the starting model.

To quantitatively evaluate the tolerance of Elastic Dynamic Matching FWI (E-DMFWI) to initial model error under varying low-frequency constraints, we introduced a controlled 4% uniform velocity slowdown to a legacy WAZ-derived velocity model. This magnitude of perturbation

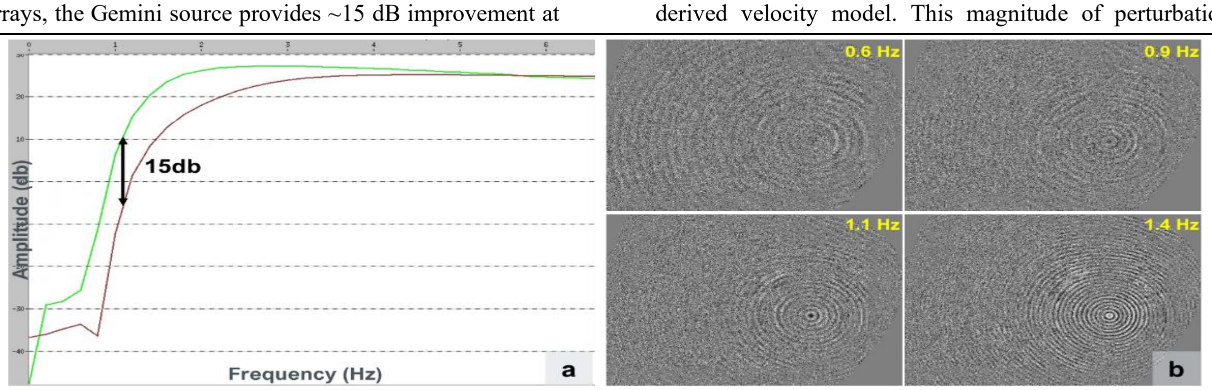

Figure 1: (a) Spectrum comparison of Gemini source (green) with conventional air gun (red), and (b) phase rings at different frequencies of a Gemini node gather.

represents realistic error scenarios encountered in practical workflows.

Three inversion experiments were conducted using identical acquisition geometry and elastic modeling parameters but different starting frequencies:

- Starting frequency 1.6 Hz (air-gun equivalent)
- Starting frequency 1.0 Hz
- Starting frequency 0.6 Hz (Gemini source)

The first experiment simulated a conventional air-gun acquisition scenario by initiating inversion at 1.6 Hz. As shown in Figure 2b, the inversion diverged rapidly. Accumulated velocity errors at shallow depth resulted in cycle skipping, and the inversion failed to produce coherent large-scale background corrections. Instead of systematic top-down positive updates, the perturbations became spatially unstable, particularly in the shallow section. This behavior is consistent with the limited tolerance of higher starting frequencies to background model bias. Even though the imposed 4% slowdown is moderate, the cumulative traveltime misalignment at 1.6 Hz exceeded the allowable phase alignment threshold, leading to unstable gradient directions and incorrect updates.

In the second experiment, inversion was initiated at 1.0 Hz. As shown in Figure 2c, the lower starting frequency improved stability relative to the 1.6 Hz case. The inversion successfully corrected much of the background bias in the sediment section and began resolving some smaller salt features. The updates extended deeper into the model compared with the previous case. However, cycle skipping effects persisted beneath larger salt bodies and in deeper target zones. The velocity corrections were incomplete in these regions, and deeper carbonate layers remained poorly reconstructed. While 1.0 Hz improved convergence, it did not fully stabilize the inversion under substantial structural complexity.

The third experiment utilized sub-Hertz data, initiating inversion at 0.6 Hz to simulate the bandwidth available from the Gemini source. The results, shown in Figure 2d, demonstrate a fundamentally different behavior. The inversion consistently corrected the imposed background bias from top to bottom. The positive velocity perturbations are coherent and spatially continuous, indicating stable gradient directions. Importantly, the inversion reconstructed deeper carbonate layers that were smoothed out in the initial model. The updates beneath major salt bodies remained stable, and no divergence was observed in the shallow section.

Compared to the higher-frequency starts, the sub-Hertz inversion exhibited significantly broader tolerance to initial model error.

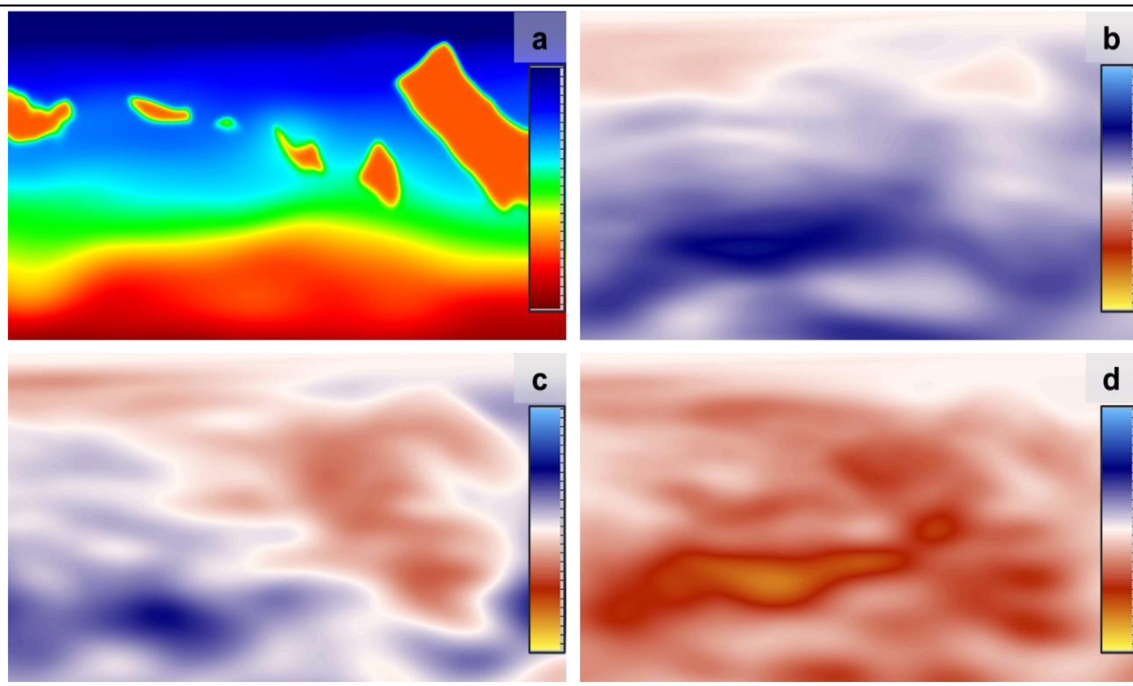

Figure 2: Initial model tolerance test. (a) A legacy salt model which is used to build the initial model for the test by scaling it down 4%. (b) E-DMFWI update with starting frequency of 1.6 Hz; (c) E-DMFWI update with starting frequency of 1 Hz; (c) E-DMFWI update at starting frequency of 0.6 Hz, it captures the slow perturbation from top down to the carbonate fast velocity which was smoothed out in the initial model

Gemini-Enabled Sub-Hertz Elastic FWI for Robust Subsalt Velocity Model Building

Direct Salt Reconstruction from Sediment Models

In the Gulf of America, the feasibility of reconstructing salt geometry directly through full-waveform inversion—without prior explicit salt interpretation—has long been debated. Conventional workflows typically rely on manual interpretation of top-of-salt and base-of-salt horizons, followed by sediment flood and salt flood migrations to progressively refine salt geometry. This process is not only time-consuming but also sensitive to illumination limitations and interpretation bias, particularly beneath complex canopy structures.

While previous synthetic studies have suggested that salt bodies may be recoverable when starting frequencies approach 0.5 Hz, practical field validation has remained limited due to insufficient low-frequency content in conventional air-gun acquisitions. The availability of ultra-low frequency data down to 0.6 Hz from the Gemini source provides an opportunity to test this concept using real OBN field data.

To evaluate this feasibility, we designed a controlled field experiment based on a legacy WAZ-derived velocity model (Figure 3a). The shallow salt bodies were deliberately removed from this model to generate a sediment-only starting model (Figure 3b). This starting model represents an intentionally biased scenario where no salt is present, forcing the inversion to reconstruct salt geometry purely from data-driven updates.

E-DMFWI was then applied using a frequency range of 0.6–1.5 Hz.

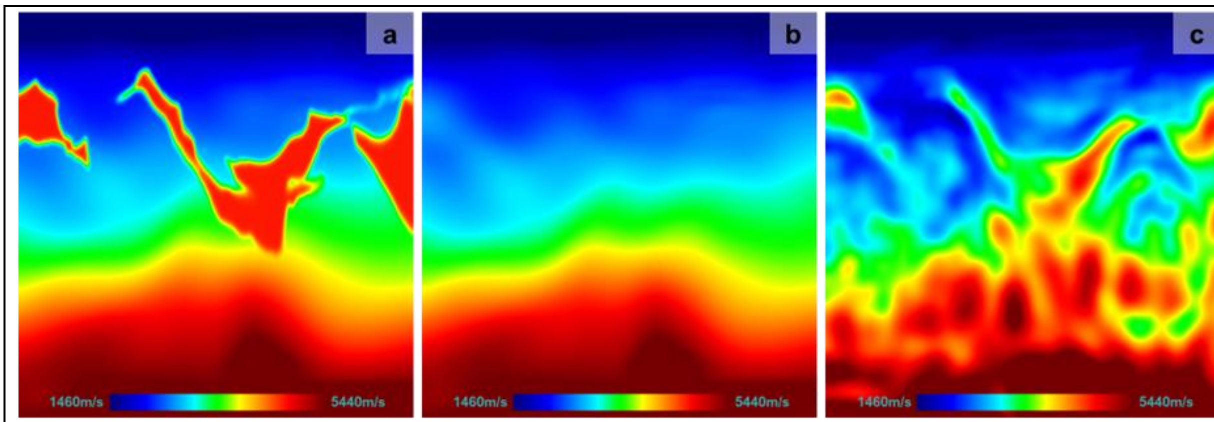

Figure 3: A legacy velocity model (a) to be used to build the initial model by removing the shallow salt (b) and (c) is the E-DMFWI output model

The inversion results, shown in Figure 3c, demonstrate that the primary salt bodies were rebuilt from the sediment-flood starting model. The reconstructed salt volumes exhibit coherent large-scale geometry, correct positioning relative to surrounding sediment, and recovered salt-sediment velocity contrast. Although fine-scale internal salt details are not fully resolved at this frequency band, the main structural framework of the salt canopy is clearly recovered.

The reconstructed salt geometry remains lower in resolution compared to interpretation-driven models, as expected, since inversion is initiated from ultra-low frequencies and only extended to 1.5 Hz in this test. However, the ability to recover the first-order salt structure directly from sediment velocities confirms that sub-Hertz data provide sufficient kinematic sensitivity to large velocity contrasts.

Subsalt Velocity Stabilization in Real Sparse OBN Projects

Having demonstrated the increased tolerance to initial model errors and the feasibility of salt reconstruction using sub-Hertz data, we now evaluate the impact of ultra-low-frequency acquisition in a practical project where a reasonably accurate starting velocity model already exists.

The comparison focuses on a line crossing the boundary between the Amendment Phase 2 and Phase 4 surveys. Both datasets share similar geology and were initialized from legacy WAZ-derived velocity models. The key difference lies in the starting frequency: Phase 2 used conventional air-gun acquisition with inversion starting at 1.6 Hz, whereas Phase 4 used the Gemini source, enabling inversion to start at 0.6 Hz. This provides a controlled field comparison isolating the impact of ultra-low-frequency bandwidth.

Figure 4a shows the 6 Hz E-DMFWI velocity model from Phase 4 with the corresponding FWI-derived reflectivity (FDR) and compares it with the 20 Hz E-DMFWI model and FDR from Phase 2. The large-scale structural framework is consistent between the two models, with similar salt geometries and subsalt basin configurations, demonstrating the robustness of E-DMFWI for Amendment OBN acquisitions. However, the sub-Hertz workflow in Phase 4 shows systematic improvements, including better intra-salt velocity definition, sharper salt–sediment velocity contrasts, clearer delineation of mini-basin boundaries, and improved resolution of Mesozoic features. These improvements are particularly evident in the Mesozoic structures highlighted by the yellow arrows in Figure 4.

Conclusions

We have demonstrated that the integration of advanced acquisition technology and robust inversion algorithms fundamentally improves subsalt velocity model building in the Gulf of America. The availability of ultra-low frequency data down to 0.6 Hz from the Gemini source significantly expands the convergence basin of Elastic Dynamic Matching FWI (E-DMFWI). Starting inversion below 1 Hz increases tolerance to initial velocity model inaccuracies, enables coherent background correction from top to base, and, in controlled tests, allows reconstruction of major salt geometries directly from sediment-flood starting models. These capabilities reduce dependency on highly accurate interpreted starting models and mitigate the risk of cycle skipping in complex salt environments.

In practical production scenarios, even when starting from reasonably accurate legacy-derived models, sub-Hertz acquisition stabilizes subsalt velocity updates and improves intra-salt and mini-basin definition. The resulting velocity models produce more coherent and better-focused RTM images beneath complex salt bodies compared to conventional 1.6 Hz workflows. These results confirm that acquisition–imaging confluence—combining sub-Hertz OBN acquisition with elastic dynamic matching inversion—provides a viable and impactful pathway for next-generation subsalt exploration.

Acknowledgements

We thank TGS MultiClient for permission to present these results.

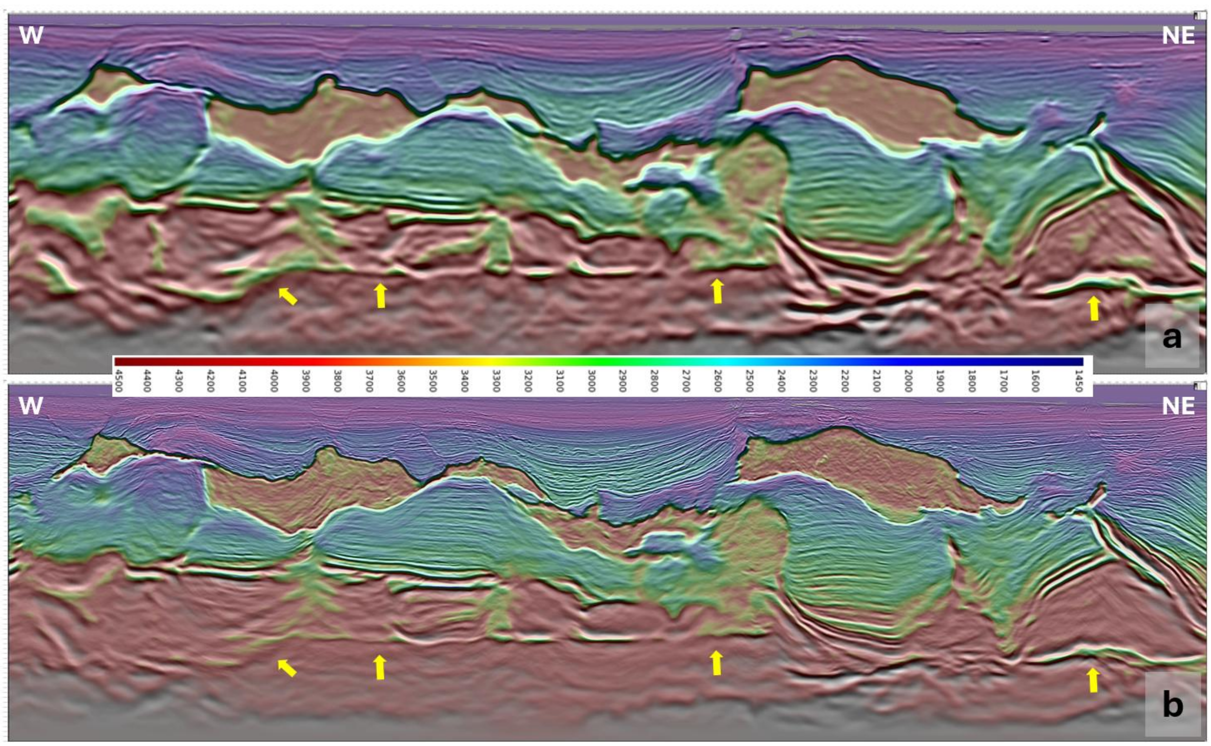

Figure 4: (a) Amendment Phase 4 6Hz E-DMFWI model and FDR (b) Amendment Phase 2 20Hz E-DMFWI model and FDR